



**COMPLETE AND INCOMPLETE FUSION STUDIES IN
SOME
 $^{16}\text{O} + ^{165}\text{Ho}$ SYSTEMS AT VARIOUS ENERGIES.**

By
Tesfahun Markos

A THESIS SUBMITTED IN PARTIAL FULFILLMENTS OF THE REQUIREMENTS
FOR THE DEGREE OF MASTER OF SCIENCE IN PHYSICS

AT
ADDIS ABABA UNIVERSITY
ADDIS ABABA, ETHIOPIA

ADDIS ABABA UNIVERSITY
DEPARTMENT OF
PHYSICS

Advisor:

Prof.A.K. Chaubey

Examiner:

Prof. P. Singh

Examiner:

Dr. Tilahun Tesfaye

ADDIS ABABA UNIVERSITY

Author: Tesfahun Markos

Date: 2014

**TITLE: COMPLETE AND INCOMPLETE FUSION STUDIES IN
SOME $^{16}O + ^{165}Ho$ SYSTEMS AT VARIOUS ENERGIES.**

Department: **Physics**

Degree: **M.Sc** Convocation:

Year: 2014

Permission is herewith granted to Addis Ababa University to circulate and to have copied for non-commercial purposes, at its discretion, the above title upon the request of individuals or institutions.

Signature of Author

THE AUTHOR RESERVES OTHER PUBLICATION RIGHTS, AND NEITHER THE THESIS NOR EXTENSIVE EXTRACTS FROM IT MAY BE PRINTED OR OTHERWISE REPRODUCED WITHOUT THE AUTHOR'S WRITTEN PERMISSION.

THE AUTHOR ATTESTS THAT PERMISSION HAS BEEN OBTAINED FOR THE USE OF ANY COPYRIGHTED MATERIAL APPEARING IN THIS THESIS (OTHER THAN BRIEF EXCERPTS REQUIRING ONLY PROPER ACKNOWLEDGMENT IN SCHOLARLY WRITING) AND THAT ALL SUCH USE IS CLEARLY ACKNOWLEDGED.

Acknowledgments

Before all, I thank almighty God that he made it all possible in whatever situation. Then it is my pleasure to extend my deepest and sincere gratitude to my advisor Prof. A. K. Chaubey for his valuable assistance, guidance, supervision, patience with all my questions, suggestions and for Providing necessary materials for the fulfillment of this thesis. I am also thankful to Addis Ababa University (Department of Physics) for the support provided and for extending facilities for carrying out this thesis

Table of Content

Acknowledgments	i
Table of contents	ii
List of Tables	iii
List of Figures	iv
Abstract	v
1. Introduction	1
2. Nuclear Reaction Theories	3
2.1 Types of nuclear reactions.	5
2.2 Reaction Cross-section	6
2.3 Reaction Mechanisms	9
2.3.1 Direct Reactions	11
2.3.2. Compound nucleus	13
2.3.3 Pre-equilibrium Reaction	16
2.4 Heavy ion Reactions	16
2.4.1 Types and properties	17
2.4.2 Complete Fusion of HI	20
2.4.3 Incomplete Fusion of HI	22
2.5 Nuclear Reactions and Models	24
2.5.1 Intra-nuclear Cascade Model	24
2.5.2 Harp-Miller-Berne Model	24
2.5.3 The Exciton Model	25
2.5.4 The Hybrid Model	26
2.5.5 Geometry Dependent Hybrid Model	27
3. THE COMPUTER CODES AND FORMULATION	28
3.1 Analysis with computer codes	28
3.1.1 Analysis with computer code PACE	30
4. Result and discussion	31
5. Conclusion	41
References	42

List of tables

Table 4.1: List of reactions identified along with the residues	31
Table 4.2. Theoretical and measured cross-sections for the reaction $^{165}\text{Ho}({}^6\text{O}, 3n){}^{178}\text{Re}$	32
Table 4.3. Theoretical and measured cross-sections for the reaction $^{165}\text{Ho}({}^6\text{O}, 4n){}^{177}\text{Re}$	33
Table 4.4. Theoretical and measured cross-sections for the reaction $^{165}\text{Ho}({}^6\text{O}, 5n){}^{176}\text{Re}$	34
Table 4.5. Theoretical and measured cross-sections for the reaction $^{165}\text{Ho}({}^6\text{O}, \alpha n){}^{176}\text{Ta}$	35
Table 4.6. Theoretical and measured cross-sections for the reaction $^{165}\text{Ho}({}^6\text{O}, \alpha 2n){}^{175}\text{Ta}$	36
Table 4.7. Theoretical and measured cross-sections for the reaction $^{165}\text{Ho}({}^6\text{O}, \alpha 3n){}^{174}\text{Ta}$	37
Table 4.8. Theoretical and measured cross-sections for the reaction $^{165}\text{Ho}({}^6\text{O}, \alpha 4n){}^{173}\text{Ta}$	38
Table 4.9. Theoretical and measured cross-sections for the reaction $^{165}\text{Ho}({}^6\text{O}, 3\alpha 3n){}^{166}\text{Tm}$	39

List of figures

Fig. 2.1. Diagram representation of nuclear reaction	3
Fig. 2.2. Discret values of impact parameter in cross-section	8
Fig. 2.3. Direct, pre-compound and compound nucleus contributions to a nuclear Reaction.....	10
Fig. 2.4. Neutron emission spectrum showing contributions of different reaction mechanisms in Nuclear reaction	11
Fig.2.5. Classical picture of heavy ion interaction showing the trajectories corresponding close, grazing, peripheral and distant collisions	19
Fig.2.6. Model of CF of heavy ion.....	20
Fig. 2.7. Model of ICF of heavy ion.....	22
Fig.4.1 Excitation function for the $^{165}\text{Ho} (^{16}\text{O}, 3\text{n})^{178}\text{Re}$ reaction.....	32
Fig.4.2 Excitation function for the $^{165}\text{Ho} (^{16}\text{O}, 4\text{n})^{177}\text{Re}$ reaction.....	33
Fig.4.3 Excitation function for the $^{165}\text{Ho} (^{16}\text{O}, 5\text{n})^{176}\text{Re}$ reaction.....	34
Fig.4.4 Excitation function for the $^{165}\text{Ho} (^{16}\text{O}, \alpha\text{n})^{176}\text{Ta}$ reaction.....	35
Fig.4.5 Excitation function for the $^{165}\text{Ho} (^{16}\text{O}, \alpha 2\text{n})^{175}\text{Ta}$ reaction.....	36
Fig.4.6 Excitation function for the $^{165}\text{Ho} (^{16}\text{O}, \alpha 3\text{n})^{174}\text{Ta}$ reaction.....	37
Fig.4.7 Excitation function for the $^{165}\text{Ho} (^{16}\text{O}, \alpha 4\text{n})^{173}\text{Ta}$ reaction.....	38
Fig.4.8 Excitation function for the $^{165}\text{Ho} (^{16}\text{O}, 3\alpha 3\text{n})^{166}\text{Tm}$ reaction.....	39

Abstract

An attempt has been made to study the complete and incomplete fusion reaction of ^{16}O induced reactions at variable energies (72MeV to 105MeV). Excitation functions (EFs) of various reaction products populated via CF and/or ICF of ^{16}O projectile with ^{165}Ho target were calculated using the statistical model code PACE4. The theoretically calculated EFs were compared with the experimentally measured values obtained from the data given in a material by Kamal Kumar et al. [12], which is conducted by the experimental details given in Ref [12]. The theoretically measured values are in general found to be in good agreement with the experimentally measured excitation functions (EFs) for non- α emitting channels in the present target projectile system. However, for α -emitting channels, the measured EFs were higher than the predictions of the theoretical model code PACE4, which may be credited to incomplete fusion reactions at these energies.

1. Introduction

At present days the study of the interaction of two heavy ions has acquired a central place in nuclear physics research[1, 6]. Again different papers are also being published. This is possible with the availability of the accelerated beams of heavy ions [11]. Recent studies show that there are different reaction mechanisms in heavy ion reactions at energies around the coulomb barrier to well above it. These reaction mechanisms have been discussed in recent papers [1, 6, 11].

The formation of compound nucleus is the dominant process at lower excitation energies. In Compound nucleus formation reactions, the projectile is captured by the target nucleus and its Energy is shared and re-shared among the nucleons of the compound nucleus until it reaches a State of statistical equilibrium. After a time much longer than the time required by the projectile to cross the nucleus, a nucleon or a group of nucleons near the surface may, by a statistical fluctuation, receive enough energy to escape or evaporate from the composite system.

At moderate excitation energies, however, there may be indications that pre-equilibrium emission(where there is emission of a particle long before the attainment of statistical equilibrium) also contributes to the reaction processes. Late experimental studies [6, 12] have shown that complete fusion and incomplete fusion reactions play important roles in heavy ion reactions. In the case of complete fusion (CF) reaction process of the projectile with the target, the projectile completely fuses with the target nucleus. Or, the entire momentum of the projectile is transferred to the target nucleus. In the case of incomplete fusion reaction, only a part of the projectile fuses with the target nucleus and the rest of it is going into the beam direction with almost the same velocity as that of incident ion beam. In this case, the fraction of the momentum transferred depends on the mass of the fused fragment. Fractional momentum transfer, in which the residue formed as a result of ICF of projectile travels to a lower range in a given medium.

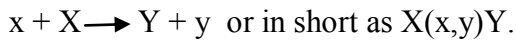
The main objective of this study is to study complete and incomplete reaction mechanisms in a heavy target nucleus. This is accomplished by the study of the excitation

functions of the residues produced in the system $^{16}\text{O}+^{165}\text{Ho}$. This and other measurements [12] have shown the importance of complete and incomplete fusion as well as of pre-equilibrium emission processes in heavy ion reactions at energies around the coulomb barrier. The excitation functions for eight reactions produced in the $^{16}\text{O} + ^{165}\text{Ho}$ system have been measured in the energy range $\approx 72-105\text{MeV}$ to study complete fusion and incomplete fusion reactions in heavy ion reactions. Recently [12], it has been observed that the incomplete fusion becomes more and more dominant as the projectile energy increases.

The present experimental values [12] are taken from experiments done using the $^{16}\text{O}^{7+}$ beam at the inter university Accelerator center (IUAC), New Delhi, India. The measured excitation functions are compared with theoretical calculations obtained using the computer programs PACE4[12] which evaluates the cross-sections for evaporation residues formed in the complete fusion reaction process of the projectile with the target without taking the incomplete fusion reaction process into account.

2. Nuclear Reaction Theories

A nuclear reaction takes place, when an incident ion of sufficient energy interacts with a target nucleus. When a nucleon or a combination of nucleons come closer to a nucleon or a nucleus (with in the short range nuclear force), the interaction takes place. In this interaction, there may transfer of energy, momentum (linear as well as angular) and also exchange of nucleons (mass transfer). Such types of interactions are called nuclear reactions. A projectile may give (stripped off) nucleons to the target Nucleons or it may pick up some nucleons from target. In general nuclear reaction is expressed or represented as:



Where X is the target, x is the projectile, Y is the residual system and y is the emitted particle.

In nuclear reaction, some new systems are evolved and some particles are emitted. It is possible to define nuclear reaction as the interaction between nucleon and nucleon, nucleon and nucleus, and heavy ions and heavy ions.

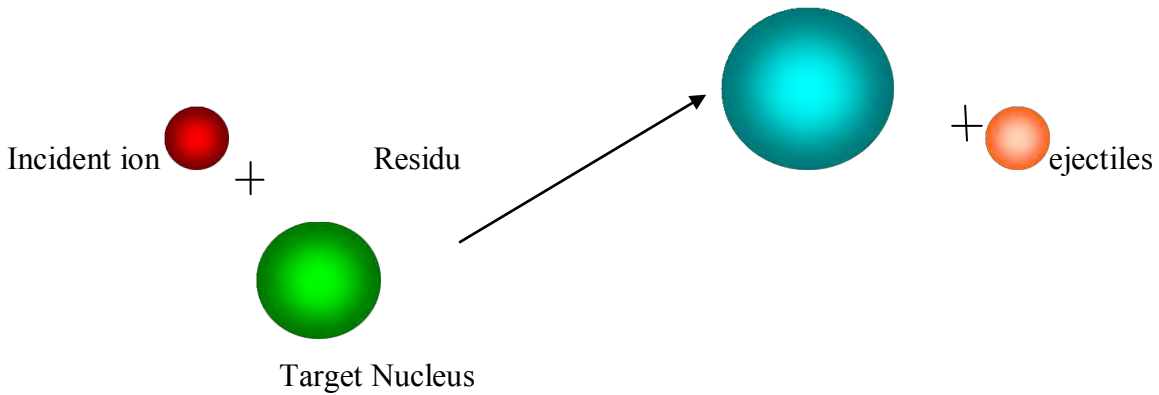


Fig. 2.1. diagram representation of nuclear reaction .

The study of nuclear reactions is one important field of research to understand nuclear reaction mechanism and other nuclear structure properties. Most of the known nuclear reactions are produced by exposing different materials to a beam of accelerated nuclear particles. For nuclear reactions to occur the energy must be high enough to overcome the

natural repulsion between the protons. This energy barrier is called the Coulomb barrier. If the energy is below the barrier, their action will bounce off each other.

When a collision occurs between the incident particle and a target nucleus, either the beam particle scatters elastically having the target nucleus in its ground state or the target nucleus is internally excited and subsequently decays by emitting radiation or nucleons. A nuclear reaction is described by identifying the incident particle, target nucleus, and reaction products.

Nuclear reactions are subject to the conservation laws [1, 8]. These laws are the conservation of energy, momentum (linear and angular), total charge, mass number, spin, parity, baryon number, Lepton number, etc.

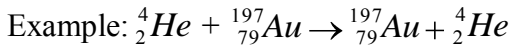
The Q-value of any reaction is an important parameter that should be taken into consideration while studying nuclear reactions. It is defined as the energy released or absorbed in the reaction, given as:

$$Q = (M_x + M_a - M_y - M_b) C^2 \quad (2.1)$$

Where M_x is the mass of the target, M_a is the mass of the projectile, M_y is mass of the residue, M_b is the mass of the emitted particle and C is the speed of light in vacuum.

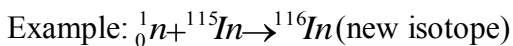
2.1 Types of nuclear reactions.

a) Elastic scattering: is a type of nuclear interaction where projectile is scattered without appreciable energy loss. No excitation of nucleus takes place. In this type of reaction small energy loss is required to conserve the momentum. Target nucleus and the projectile both remain in the initial quantum mechanical state. That is no excitation of target nucleus.



b) Inelastic scattering: In this type of nuclear reactions, there is an appreciable energy loss and the target nucleus is in the excited state after reaction and it comes to ground state by emitting gamma radiation. Example: ${}_1^1\text{H} + {}_3^7\text{Li} \rightarrow {}_3^7\text{Li}^* \rightarrow {}_3^7\text{Li} + \gamma$

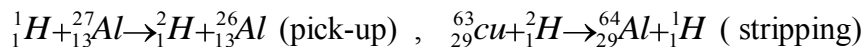
c) Radioactive capture: is also other type of nuclear reaction where the projectile is captured (absorbed) by the target nucleus such that the energy of excitation is not very high. Target nucleus after capturing projectile is converted into New isotope or New element.



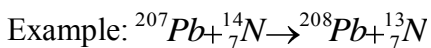
d) Disintegration of nucleus: is a nuclear reaction type whereby there is emission of different particles because depending upon the energy of the projectile the system may disintegrate. Here different residual systems are possible with different combination of emitted particles, and also low energy γ -rays may be associated.

e) Many body interaction: it is a type of nuclear reaction in which there is emission of more than one particle from compound nucleus.

f) Stripping and pickup reaction: A reaction in which a projectile is stripped off a nucleon or picks up(takes) a nucleon from target. These reactions induced by heavy ions are of both types. Formation of compound nucleus and also direct reactions.



g. Heavy ion reaction: reaction in which projectile is heavy ion (heavier than alpha).



h). Elementary particle reactions: involves a type of reaction in which there is a production of elementary particles. high energy beam of protons. $\sim 150\text{Mev}$.

Example: $p + p \rightarrow p + n + \pi^+$

i). Nuclear fusion and fission reactions are other types of nuclear reactions. In fusion reaction there is a combination of two nuclei to form a more massive nucleus where as in fission reaction there is a disintegration of a heavy nucleus into different fragments.

2.2 Reaction Cross-section

Reaction cross-section is the most important quantity in nuclear reaction study. The reaction cross-section is a measure of the probability of the reaction. Since interactions in a nuclear reaction take place with individual target nuclei independently of each other, it is useful to refer to the probability of a nuclear reaction to one target nucleus.

It is defined in terms of number of events produced (number of particles emitted after reaction) for separate number of incident particles. It can be also defined in terms of number of nuclei transformed per specific number of incident particles. In fact nuclear reaction cross section is the effective area of the nuclei shown to the incident beam or it the effective area of the nuclei as seen by the incident beam. If the incident particles pass through this area, the interaction will take place. It may be in many cases equal to geometrical cross sectional area (πR^2) or it may be more or less than (πR^2). It is the probability that an interaction may occur when a single particle is shot perpendicularly at a target having one nucleus per unit area this is represented by symbol σ .

or $\sigma = \frac{\text{number of particular types of events per unit time per nuclei}}{\text{number of incident particles per unit time per unit area}}$

the dimensions of σ is that of area. so it is measured in terms of cm^2 or m^2 . it is also measured by another unit called Barn. $1 \text{ barn} = 10^{-24} \text{cm}^2$ or 10^{-28}m^2

If N is the reaction product and I is the incident particles, then the probability of reaction is given as:

$$\sigma = \frac{N}{I} \quad 2.2$$

if σ is the effective area of the nucleus as seen by the projectile, and if n is the number of nuclei present per unit volume of target, S is surface area of target, Δx is the thickness of the target, then the effective area of nuclei present in the target is equal to $= \sigma n S \Delta x$.

That is $n S \Delta x$ is the total number of nuclei in the target and $S \Delta x$ is volume of the target.

Therefore the ratio of the effective area present in that target nuclei to the surface area of target gives the probability of the reaction. Or

Probability of reaction = $\frac{\sigma n S \Delta x}{S}$. this implies that,

$$\frac{N}{I} = \frac{\sigma n S \Delta x}{S} \text{ and } \sigma = \frac{N}{\left(\frac{I}{S}\right) n S \Delta x} . 2.3$$

The reaction cross-section for any reaction can be measured by measuring N (emitted particles per second). $n S \Delta x$ can be calculated from known size of target, and known value of $\frac{I}{S}$.

Also for total cross section, we can have an expression from total attenuation of incident beam. If I_0 is the incident beam and dI is the attenuation of beam by all the processes, so that I is the emergent beam after passing through the target. We can write it as:

$$-\frac{dI}{I} = \sigma n \Delta x , \text{ and hence, } I = I_0 e^{-\sigma n \Delta x} . 2.4$$

I is the beam intensity after passing through target of thickness „ x “ having „ n “ nuclei per unit volume. The impact parameter is an important parameter in nuclear reactions to take place, as stated earlier, and it has a connection with the reaction cross-section-the probability for nuclear reaction to take place. To see this connection, consider the projectile beam as particle wave. There will be interaction of beam with target, from classical considerations, when the impact parameter of beam is less than the nuclear radius i.e., if $b \leq R$ interaction takes place and if $b > R$ no interaction is taking place.

Angular momentum is given as $\mathbf{p} \times \mathbf{b}$. But from quantum mechanics, angular momentum is quantized and is given as $l\hbar$, where $l=0, 1, 2, \dots$ etc. From this relation we can write angular momentum as $pb=l\hbar$ or the impact parameter $b = \frac{l\hbar}{p}$ or $b = \lambda l$. Where $\lambda = \hbar/p$ is the

reduced de Broglie wave length. This clearly shows that the idea of quantization of angular momentum leads to the quantization of impact parameter. We can imagine particles of beam moving with having different quantized value of impact parameter. One can divide the particles of beam in different zones having different impact parameters. Particles moving in the central zone having $l=0$ and impact parameter $b \leq \lambda$. In the next

zone particles of impact parameter of b value $\lambda < b < 2\lambda$ having $l=1$ are moving. In the next zone particles having $l=2$ and impact parameter $2\lambda < b < 3\lambda$ are moving. In this way particles moving in l th zone will have impact parameter in between $l\lambda$ and $(l+1)\lambda$.

Geometrical area of l th zone will be:

$$\pi [(l+1)\lambda]^2 - \pi [l\lambda]^2 = \pi \lambda^2 [2l+1] \quad 2.5$$

Then the reaction cross-section, is given as $\sigma_{r,l} = \pi \lambda^2 [2l+1]$ 2.6

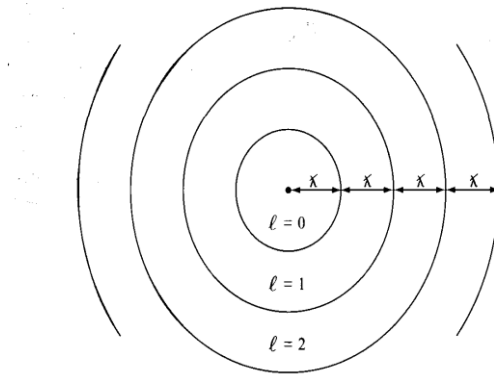


Fig. 2.2. Discrete values of impact parameter in cross-section

2.3 Reaction Mechanisms

In nuclear reaction [1], there are three mechanisms of nuclear reaction. These are direct reaction, compound nucleus reaction and pre-equilibrium reaction. The direct reaction takes place in the time the projectile takes to traverse the target nucleus ($\sim 10^{-22}$ s). In this reaction, the projectile may interact with a nucleon; a group of nucleons or with the whole nucleus and emission takes place immediately.

The compound nucleus reaction takes place when the projectile is captured by the target nucleus. In this reaction, the energy and momentum of the projectile is shared and re-shared among the nucleons of the compound nucleus until it reaches a state of statistical equilibrium. This transfer of energy and momentum takes so much time ($\sim 10^{-15}$ s) that the incoming projectile becomes part of the system because there is a thorough mixing of all the nucleons energy.

The pre-equilibrium reaction is a reaction mechanism where a particle is emitted neither immediately after the interaction of the projectile with a nucleon or with a group of nucleons of the target nucleus, as in a direct reaction, nor after a long time by the statistical decay of the compound nucleus. The projectile may share its energy among a small number of nucleons which may further interact with other nucleons, and this cascade of nucleon-nucleon interactions through which the energy of the incident particle is progressively shared among the target nucleons, a particle may be emitted long before the attainment of statistical equilibrium.

All these reactions are subject to the conservation laws of energy, momentum, mass number, spin, total charge, parity, lepton number, baryon number, etc. The relative importance of these three reaction mechanisms depends on the type of interacting particles and their relative energy.

In these different types of reaction mechanisms, after the first interactions, the nucleon may leave the nucleus immediately by a direct reaction or it may interact with a nucleon in the nucleus and start a cascade of nucleon-nucleon interaction from which pre-equilibrium emission may occur.

During this cascade, the energy is shared among an increasing number of nucleons until eventually the compound nucleus is formed. The compound nucleus may decay into the elastic or any of the reaction channels that are allowed energetically. The shape elastic and compound elastic processes combine to give the measured elastic scattering cross-section. In a similar way the direct, pre equilibrium and compound nucleus processes combine to give the inelastic cross-sections and all the other non-elastic reactions.

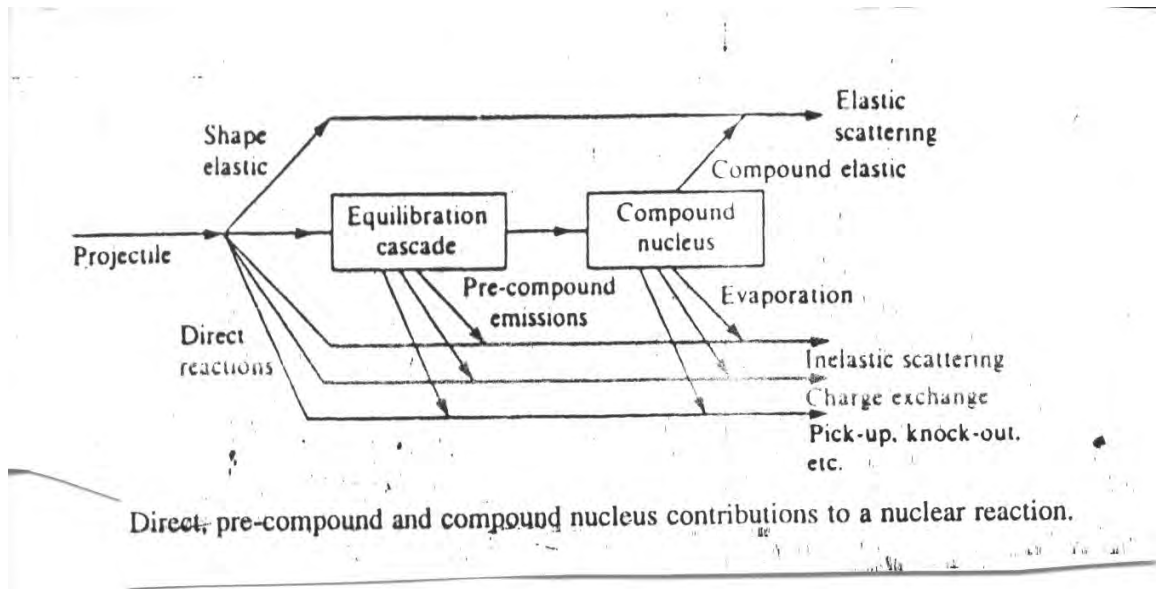


Fig. 2.3.

This shows the connection between the different reaction mechanisms.

All the above mentioned reaction mechanisms may contribute to a given reaction and an experiment may focus on one contribution or the other. To show this, consider the elastic scattering of a nucleon or a proton by a nucleus. At low energies, neutrons and protons interact very differently. Protons are repelled by the electrostatic field of the nucleus and are scattered elastically with a cross-section given by Rutherford's formula. This is a direct reaction. Low energy neutrons may be scattered by the nuclear field (this is potential scattering, or shape elastic scattering, a direct process) or may be captured to form the compound nucleus and then emitted with the same energy. This is compound elastic scattering, which is strongly affected by the structure of the compound nucleus.

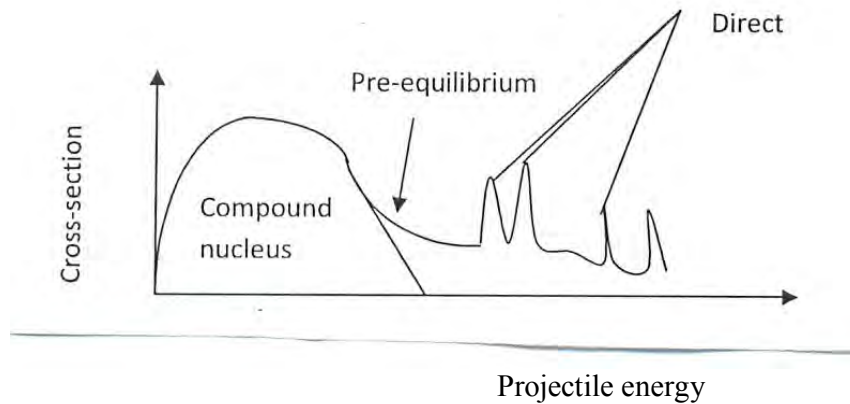


Fig. 2.4. Neutron emission spectrum showing contributions of different reaction mechanisms in nuclear reaction

2.3.1 Direct Reactions

A direct reaction [1,7] occurs when the projectile interacts primarily with the nucleons in the surface of the target nucleus. The interaction is with one or two nucleons. Energy and momentum transfer is very small and the transfer is to only few nucleons, and emission of the particle most probably is in the direction of motion of the projectile.

At the opposite extreme from compound-nucleus reactions are direct reactions, in which the incident particle interacts primarily at the surface of the target nucleus: such reactions are also called peripheral processes. As the energy of the incident particle is increased, its de Broglie wavelength decreases. Until it becomes more likely to interact with a nucleon-sized object than with a nucleus-sized object. A 1-MeV incident nucleon has a de Broglie wavelength of about 4fm, and thus does not "see" individual nucleons; it is more likely to interact through a compound-nucleus reaction. A 20-MeV nucleon has a de Broglie wavelength of about 1fm and therefore may be able to participate in direct processes. Direct processes are most likely to involve one nucleon or very few valence nucleons near the surface of the target nucleus.

Direct reactions become more probable as one increases the energy of the incident particle: the wavelength associated to the particle decreases and localized areas of the nucleus can be "probed" by the projectile. In this context, peripheral reactions, where only a few nucleons of the surface participate become important. Direct reactions happen during a time of the order of 10^{-22} s. Reactions with formation of compound nuclei can be

up to six orders of magnitude slower. A reaction type at a given energy is not necessarily exclusive; the same final products can be obtained, part of the events in a direct way, other parts through the formation and decay of a compound nucleus.

There are two characteristic types of direct reactions. In the first the incident particle scatters in elastically and the transferred energy is used to excite a collective mode of the nucleus. Rotational and vibration bands can be studied in this way. The second type involves a modification in the nuclear composition. Examples are transfer of nucleons, as pick-up and stripping reactions. An important reaction of the latter kind is a knock-out reaction where the incident particle knocks out a particle of the target nucleus and continues in its path, resulting in three reaction products. Reactions with nucleon exchange can also be used to excite collective states. An example is a pick-up reaction where a projectile captures a neutron from a deformed target and the product nucleus is in an excited state belonging to a rotational band. Direct reactions exhibit a peculiar form of angular distribution, which allows us to extract information on the reaction mechanism with the employment of simple. Typical examples are the stripping reactions (d,n) and (d,p), where the angular distribution of the remaining nucleon presents a forward prominent peak and smaller peaks at larger angles, with the characteristic aspect of a diffraction figure.

The main characteristics of direct reactions are: first the emission of much larger number of high energy particles than expected on the basis of evaporation model. Second, the angular distribution of emitted particles shows a forward peaking. This is may be because the direct reaction takes place with surface nucleons. The third main characteristic of direct reaction is a monotonic change of cross-section with energy, no resonances are observed. Direct reactions take place, generally, at higher energies where compound nucleus probability is very small.

2.3.2. Compound nucleus

Suppose an incident particle enters a target nucleus with an impact parameter small compared with the nuclear radius. It then will have a high probability of interacting with one of the nucleons of the target, possibly through a simple scattering. The recoiling struck nucleon and the incident particle (now with less energy) can each make successive collision with other nucleons, and after several such interactions. The incident energy is shared among many of the nucleons of the combined system of projectile + target. The average increase in energy of any single nucleon is not enough to free it from the nucleus, but as many more-or-less random collisions occur. There is a statistical distribution in energies and a small probability for a single nucleon to gain a large enough share of the energy to escape, Much as molecules evaporate from a hot liquid. Such reactions have a definite intermediate state, after the absorption of the incident particle but before the emission of the outgoing particle (or particles). This intermediate state is called the compound nucleus.

When a low energy neutron (< 50 Mev) enters the range of nuclear forces it can be scattered or begin a series of collisions with the nucleons [7]. The products of these collisions, including the incident particle, will continue in their course, leading to new collisions and new changes of energy. During this process one or more particles can be emitted and they form with the residual nucleus the products of a reaction that is known as pre-equilibrium.

At low energies, the largest probability is the continuation of the process so that the initial energy is distributed among all nucleons, with no emitted particle. The final nucleus with $A + 1$ nucleons has an excitation energy equal to the kinetic energy of the incident neutron plus the binding energy the neutron has in the new, highly unstable, nucleus [4]. It can, among other processes, emit a neutron with the same or smaller energy to the one absorbed. The de-excitation process is not necessarily immediate and the excited nucleus can live a relatively long time. We say that there is, in this situation, the formation of a compound nucleus as intermediary stage of the reaction. In the final stage the compound nucleus can evaporate one or more particles. In our notation, for the most common

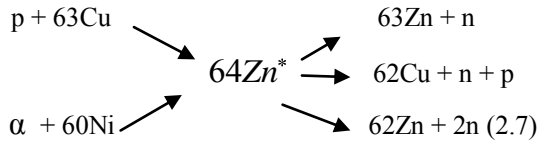
situation in which two final products are formed (the evaporated particle plus the residual nucleus or two fission fragments, etc.) we write:



The asterisk indicating that the compound nucleus C is in an excited state.

The compound nucleus lives long enough to "forget" how it was formed and the de-excitation to the final products b and B only depends on the energy, angular momentum and parity of the quantum state of the compound nucleus. An interesting experimental verification was accomplished by S. N. Ghoshal in 1950 [5]. He studied

two reactions that take to the same compound nucleus, ^{64}Zn of three different forms of decay, as shown below:



If the idea of the compound nucleus is valid and if one chooses the energy of the proton and of the incident α -particle to produce the same excitation energy, then the cross section for each one of the three exit channels should be independent of the way the compound nucleus is formed. That is, the properties of the compound nucleus do not have any relationship with the nuclei that formed it.

The angular distribution of fragments, or evaporated particles, of a compound nucleus should be isotropic in the center of mass, and this is verified experimentally. However, the total angular momentum is conserved and cannot be "forgotten". Reactions with large transfer of angular momentum, as when heavy ions are used as projectiles, can show a non-isotropic angular distribution in the center of mass system.

The occurrence of a nuclear reaction in two stages allows the cross section for a reaction $A(a,b)B$ to be written as the product, $\sigma(a,b) = \sigma_c(a,A)P(b)$; where $\sigma_c(a,A)$ is the cross section of formation of the compound nucleus starting from the projectile a and the target A and $P(b)$ is the probability that the compound nucleus emits a particle b leaving a

residual nucleus B. If the quantum numbers of entrance and exit channels are well specified, i.e., if the reaction begins at an entrance channel α , and ends at an exit channel β , one can write:

$$\delta(\alpha;\beta) = \delta_c(\alpha)P(\beta). \quad (2.8)$$

We can associate the probability $P(\beta)$ to the width Γ_β of the channel β and write:

$$P(\beta) = \frac{\Gamma_\beta}{\Gamma} \quad (2.9)$$

Where Γ is the total width, that is, $\tau = \frac{\hbar}{\Gamma}$ is the half life of disintegration of the compound nucleus. Eq. 29, just expresses the fact that the decay probability through channel β is the decay rate through that channel divided by the total decay rate. In the competition between the several channels β , the nucleons have clear preference over the γ radiation whenever there is available their emission and among the nucleons the neutrons have preference as they do not have the Coulomb barrier as an obstacle. Thus, in a reaction where there is no restriction for neutron emission we can say that

$$\Gamma \approx \Gamma_n \quad (2.10)$$

Where Γ_n includes the width for the emission of one or more neutrons. The study of the function $P(\beta)$ is done in an leads to results in many evaporation model that aspects similar to the evaporation of molecules of a liquid, with the energy of the emitted neutrons having the form of a Maxwell-Boltzmann distribution

$$I(E) \approx E \exp\left(-\frac{E}{\theta}\right) dE \quad (2.11)$$

With I measuring the amount of neutrons emitted with energy between E and $E + dE$. The quantity θ , with dimension of energy, has the role of a nuclear temperature.

The Weisskopf-Ewing theory

At low incident energies the compound nucleus states are excited individually and each produces a resonance in the cross section that may be described by the Breit-Winger theory [1]. As the incident energy increases compound nucleus states of higher energy are excited and these are closer to gather and of increasing width. Eventually they over lapp and it is no longer possible to identify the individual resonances.

2.3.3 Pre-equilibrium Reaction

Pre-equilibrium reaction [1] is neither direct nor compound nucleus reaction. In this type of reactions particles are emitted after the first stage of a nuclear interaction (direct reaction) but long before the attainment of statistical equilibrium (compound nucleus formation). Their time scale is intermediate between the very fast direct reactions and the relatively slow compound nucleus formation. In pre-equilibrium reactions, the emission of particles from the excited target nucleus is neither by statistical decay of compound nucleus nor by the prompt emission after collision. In these reactions, the projectile shares its energy among a small number of nucleons in the target; the struck nucleons initiate a cascade of reactions with the target, at the course of which a particle can be emitted before the compound nucleus was reached a state of statistical equilibrium.

The energy of the projectile is shared among the nucleons of the target by a cascade of nucleon-nucleon interactions that excites particle-hole state of increasing complexity. A pre-equilibrium reaction corresponds to emission of an unbound particle from one of these particle-hole states when the composite nucleus is not yet equilibrated. Most pre-equilibrium reactions take place at energies high enough for it to be no longer possible to resolve the individual final state. The cross-sections are those of reactions to a continuum of final states, and the absence of fluctuations in these continuum spectra shows that to a high degree of accuracy one may assume that there are no interference effects so that pre-equilibrium cross sections can be evaluated by adding incoherently the contributions from each stage of the nucleon-nucleon interaction cascade. The total cross-section for pre-equilibrium emission is then the sum of the cross-sections for emission from each stage of the cascade.

2.4 Heavy ion Reactions

We know that ions above alpha particles are called heavy ions. Particles (projectiles) heavier than α -particles are considered as heavy particles [1, 7]. Almost every element can be produced in ionized form and an accelerated beam of any heavy ion can be produced. The complex nature of the projectile makes it possible that a number of new reactions occur, and also when the projectile fuses with the target nucleus creating a compound nucleus one has to consider the

special features of heavy ion reaction due to the large angular momentum carried in by the projectile.

At low energies two heavy ions interact only through their coulomb field, and can scatter elastically or in-elastically with coulomb excitation. Nuclear interactions can only take place if the two ion energy E_{cm} in their center of mass system is high enough to overcome the coulomb barrier,

2.4.1 Types and properties

Heavy ion reactions (with $A > 4$) can be separated into three major categories.

1) Due to their large charge, two heavy nuclei feel a strong mutual Coulomb repulsion. To produce a nuclear reaction the projectile needs enough energy to overcome the Coulomb barrier. For a very heavy target, as ^{238}U , it is necessary about 5 Mev per nucleon. Then the wavelength of the projectile is small compared with the dimensions of the nuclei and classical and semi-classical methods become useful in the description of the reaction.

2) The projectile carries a large amount of angular momentum and a good part of it can be transferred to the target in the reaction. Rotational bands with several dozens of units of angular momentum can be created. In fact, heavy ion reactions are the best suited to feed high spin levels.

3) Direct reactions and formation of compound nucleus are also common processes in reactions with heavy ions.

But some peculiarities of these are not found in reactions with projectile nucleons. One of these processes can be understood as intermediate between a direct reaction and the formation of a compound nucleus. Fusion does not occur but projectile and target pass a relatively long time under the mutual action of the nuclear forces. Nuclear matter is exchanged between both and there is a strong heating of the two nuclei, with a large transfer of kinetic energy to the internal degrees of freedom. These are the deep inelastic collisions.

The kind of process that prevails depends upon the distance of closest approach d between the projectile and target. If this distance is sufficiently large only the long range Coulomb interaction acts and, for a classical hyperbolic trajectory, d is related to the impact parameter b and to the energy E of the projectile by

$$d = \frac{a}{2} + \left[\left(\frac{a}{2} \right)^2 + b^2 \right]^{\frac{1}{2}} \quad (2.12)$$

where a is the distance of closest approach in a head-on collision. It is this is related

$$\text{to } E \text{ by } a = \frac{Z_1 Z_2 e^2}{4\pi\epsilon_0 E} \quad (2.13)$$

Experimentally, the variable under control is the energy E of the projectile and, for E sufficiently large, d can be small enough to enter the range of nuclear forces.

Collisions near this limit are called grazing collisions and are characterized by values of b_{graz} and d_{graz} . Assuming that there is always reaction when $b < b_{\text{graz}}$, the reaction cross section δ_r can be determined geometrically by $\delta_r = \pi b_{\text{graz}}^2$. The experimental determination of δ_r allows to establish the value $d_{\text{graz}} = 0.5 + 1.36 \left(A_1^{\frac{1}{3}} + A_2^{\frac{1}{3}} \right)$ showing that the distance of grazing collision is somewhat larger than that deduced from two touching spheres $(3.6 \text{ fm} > r_0 = 1.2 \text{ fm})$

When the impact parameter is close to b_{graz} one expects nuclear reactions of short duration, without the Contribution of the compound nucleus formation. Such reactions are elastic and inelastic scattering and transfer of few nucleons. When the incident energy is sufficiently high, small values of b can lead to the projectile penetrating the target. Depending on the energy and on the involved masses, the reaction can end in one of the processes below:

a) Fusion - is the preferred process when one has light nuclei and low energy. There is the formation of a highly excited compound nucleus that decays by evaporation of particles and - radiation emission, leading to a cold residual nucleus. If the energy in the CM is close to the Coulomb barrier energy the cross section of compound nucleus formation starting from two nuclei is practically equal to the reaction cross section.

b) Fission - When the compound nucleus is heavy the fission process competes strongly with the evaporation of particles in each stage of the evaporation process. A very heavy compound nucleus with large excitation energy has a very small probability of arriving to a cold residual

nucleus without fission at some stage of the de-excitation. The role of the angular momentum l transmitted to the target nucleus is also essential. The fission barrier decreases with the increase of l and for a critical value l_{crit} the barrier ceases to exist. A nucleus with angular momentum greater than l_{crit} suffers immediate fission and this is also a limiting factor in the production of super heavy elements.

c) Deep inelastic collision (DIC) - is a phenomenon characteristic of reactions involving very heavy nuclei ($A > 40$) and with an incident energy of 1MeV to 3MeV above the Coulomb barrier. In DIC the projectile and the target spend some time under mutual action, exchanging masses and energy but without arriving to the formation of a compound nucleus. The projectile escapes after transferring part of its energy and angular momentum to its internal degrees of freedom and to the target, with values reaching 100MeV and $50 \hbar$.

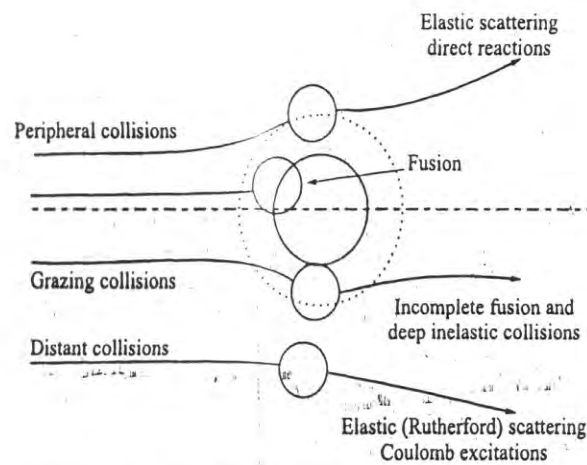


Fig. 2.5

Classical picture of heavy ion interactions showing the trajectories corresponding close, grazing, peripheral and distant collisions.

2.4.2 Complete Fusion of HI

In general Projectile is completely fused with the target nucleus, leading to the formation of an excited composite system that may decay by the emission of n, p, α etc., after attaining statistical equilibrium

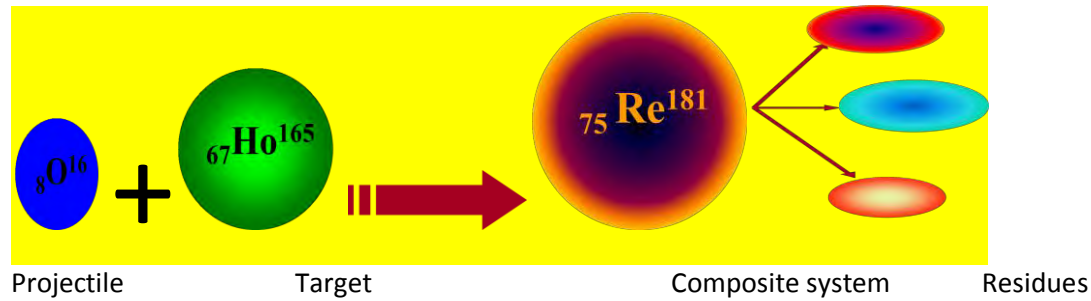


Fig. 2.6. Model of CF of heavy ion.

Heavy ion complete fusion reaction [1, 2, 9,10,12.] is a reaction where there is an entire momentum transfer from projectile to the target nucleus takes place. In this reaction, a fully equilibrated excited compound nucleus of pre-determined charge, mass and angular momentum is formed.

Heavy ion fusion reactions have been extensively studied because they offer possibility of producing nuclei with high excitation energy and high spin thus allowing study of nuclear matter in conditions which are not easily formed in other reactions. Fusion reactions have also been used to try produce super-heavy nuclei and to produce proton rich nuclei very far from the stability line. There are important features of fusion reactions. For light projectiles and low incident energies the fusion cross-section may be a considerable fraction of the reaction cross-section. The second important feature is, with increasing charge of the interacting ions the fusion probability falls abruptly. The other feature of fusion reaction is the fusion cross-section at first increases linearly with $\frac{1}{E_{CM}}$, reaches a maximum and thereafter decrease linearly with $\frac{1}{E_{CM}}$.

The detailed energy dependence of the fusion cross-section may differ quite considerably for different interacting ions forming the compound nucleus. In general, the fusion cross-section varies quite smoothly with the energy, but in the case of light systems it may show quite large oscillations. When two heavy ions fuse, they form a compound nucleus which is far from statistical equilibrium since a large fraction of its energy is in form of an orderly collective

translational motion of the nucleons of the projectile and the target. This orderly motion transforms into chaotic thermal motion through a cascade of nucleon-nucleon interactions during the thermalization of the compound nucleus. This takes some time and before reaching thermal equilibrium, nucleons or clusters of which still have energy considerably higher than their equilibrium thermal energy may be emitted into the continuum. These pre-equilibrium emissions must be taken into account to reproduce the multiplicity and the spectra of the ejectiles measured in heavy ion fusion reactions. The ejectiles emitted in a fusion reaction at rather low incident energies are detected in coincidence with the residue, of mass near to the compound nucleus, emitted at a very forward angle with a velocity about equal to that expected for a complete momentum transfer.

At higher incident energies this is no longer valid since the excitation energy of the compound nucleus is very high and it emits, before reaching statistical equilibrium, so many particles that the velocity of the residue is considerably less.

The excitation functions of several heavy ion fusion reactions depart from what is expected for purely evaporative contributions. Starting from bombarding energies only slightly above the coulomb barrier acting between the two interacting ions and seem to be satisfactorily reproduced only if emission of pre-equilibrium nucleons is taken into account. Some calculations [1] suggest that with increasing bombarding energy an increasing fraction of the excitation energy is dissipated by emitting pre-equilibrium particles (about 50% at an energy about 30 Mev/nucleon), greatly reducing the probability of forming very excited equilibrated nuclei.

2.4.3 Incomplete Fusion of HI

Only a part of the projectile fuses with the target nucleus and the rest of it is going into the beam direction with almost the same velocity as that of incident ion beam. ($^{16}\text{O} = ^{12}\text{C} + \alpha$)

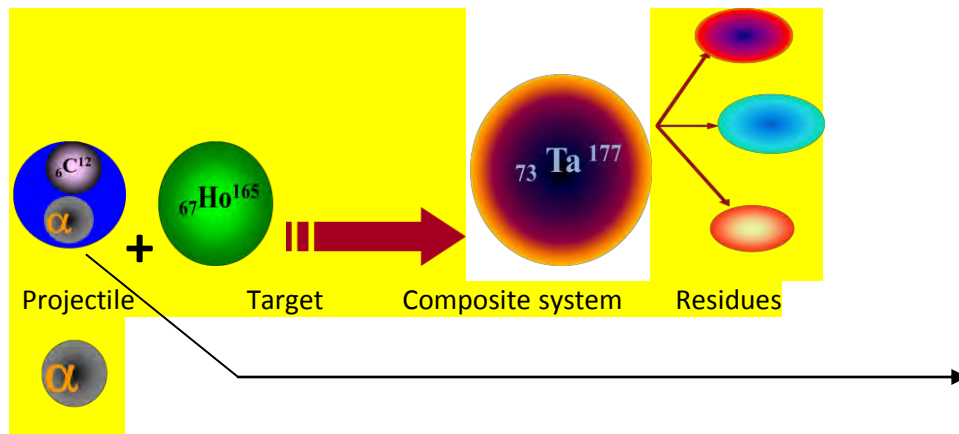


Fig. 2.7. Model of ICF of heavy ion.

In the above figure the residues are produced by the emission of neutrons, protons or α -particles. Incomplete fusion reaction [1, 6,9,10] is a reaction where fractional mass, charge and momentum of the projectile are transferred to the target nucleus due to the prompt emission of projectile fragment(s) in the forward direction with almost projectile velocity. There are various binary break-up processes. Elastic break-up with immediate emission of both fragments originating from the break-up and no excitation of the target, which may be released by coincidence experiments, inelastic break-up in which both fragments come out after the interaction, but one of them after having interacted with the target nucleus, which further de excites with emission either of particles or γ -rays, and break-up fusion or incomplete fusion in Which only one of the fragments comes out (the spectator fragment) while the other (the participant fragment) is absorbed by the target nucleus which may be considerably excited. In elastic and inelastic break-up reactions both fragments are emitted where as in break-up fusion or incomplete fusion processes only one of the fragments come out while the other is absorbed by the target nucleus. The importance of this process is revealed by the study of excitation functions of reactions induced by complex projectile.

Incomplete fusion reaction has also been observed in the interaction of light ions [1,12,13] such as ^{12}C , ^{14}N and ^{16}O with heavy targets. These ions may break-up preferentially into α -type fragments (for instance, in this work, Oxygen may break-up into ^{12}C and α -particle or ^8Be and two α -particles or ^8Be and ^8Be) where one of which further fuses with the target nucleus. The contribution of the incomplete fusion cross-sections may be separated from the complete fusion in several ways. The first evidence for such phenomena was found by measuring the angular correlation of fission fragments. Fusion reactions lead to emission of fragments at relative less angles and are the dominant contribution at all the energies considered, but, with a probability increasing with energy, almost back-to-back fragment emissions are also observed. This may only occur if, as in incomplete fusion, a momentum considerably smaller than that of the projectile is transferred to the fissioning compound nucleus.

Further experiments [1] measured the incomplete fusion cross-section by detecting the spectator fragment in coincidence with the γ -lines of the incomplete fusion residue or by measuring (by activation techniques) the recoil ranges and the angular distribution of the incomplete fusion residues. These last experiments are based on the consideration that a compound nucleus formed in an incomplete fusion reaction has, respectively, a smaller linear momentum and a larger recoil angle than a compound nucleus formed in a complete fusion process.

As a consequence the residues also have a smaller range and a larger recoil angle and both effects contribute to reduce the projection of their recoil range in the beam direction. Thus, if a residue is formed both in fusion and in an incomplete fusion, the two contributions may be separated by looking at their forward recoil range distribution. Even more effective in separating the two contributions may be angular distribution measurement. Residues of fusion reaction, especially at not too high incident energies where emission of intermediate mass fragment is quite improbable, are concentrated in a forward direction along the beam direction. Those formed in incomplete fusion processes recoil to angles appreciably different from zero.

Some of the important features of ICF are [6]:

Higher measured cross-sections than predicted by statistical models, Fractional momentum transfer, in which the residue formed as a result of ICF of projectile travels to a lower range in a given medium or incomplete momentum transfer, the threshold for ICF is not well established.

Early studies show occurrence of ICF at higher energies above 10 MeV/nucleon. Recent experimental studies have shown that ICF starts competing with CF even at energies around 5-7 MeV/nucleon i.e, just above the Coulomb barrier.

2.5 Nuclear Reactions and Models

2.5.1 Intra-nuclear Cascade Model

The Intra-nuclear cascade model [8] was first proposed by Serber and first implemented to explain the interactions of high energy neutrons with complex nuclei. In INC model the projectile enters the target nucleus with a given parameter “b”. The projectile interacts with the target nucleons after travelling a certain distance inside the target nucleus, and excites it above the Fermi Sea. Each scattered particle then travel through the nucleus interacting with the other nucleons. The INC model traces the individual nucleon trajectories in three-dimensional geometry. The trajectories of all excited particle are followed until some arbitrary energy significantly above the mean equilibrium value has been attained by the nucleon. Particles reaching the nuclear surface with sufficient energy are assumed to be emitted. When all particles of a given cascade have been traced, the total energy of the residual nuclei, its identity, and the energies and angles of the emitted particles are shared, and a new cascade with new impact parameter is calculated with help of such an approach, the time evolution of the reaction can be generated but after few collisions the actual calculations becomes too much complicated. The INC model is a realistic model but in general, the model prediction is not satisfactorily at backward angles and is some forward angles also.

2.5.2 Harp-Miller-Berne Model

In Harp-Miller-Berne model [8], the nuclear single particle states are classified according to their energies in groups or “bins” whose size ΔE is chosen to be of some convenient dimension. In the calculations, the fractional occupation of each bin is taken as function of time. This model Calculates the occupation probability of an average state in i^{th} bin as a function of time using Fermi gas distribution. At the initiation of the reaction, at the time t_0 all the levels below the Fermi energy are filled up (as the target is in ground state), and the projectile is in an excited

state. This gives the fractional occupation probability at time $\tau = \tau_0$. Two-body interactions then lead to a distribution of probabilities.

After calculating the relative probabilities of scattering into and out of each bin and the emission from bins above the particle binding energies, populations of all bins are changed accordingly. The calculation is repeated until a steady state configuration is reached. At each time during the equilibrium process the energy spectrum of emitted nucleons are calculated and a net spectrum obtained. Later by Harp and Miller in HMB model, a minor modification is suggested. They considered the nucleus to be composed of independent proton and neutron Fermi gases. Therefore, the proton and neutron occupation numbers for the single particle states of these gases completely specifies the internal configuration of the nucleus at any time. Further, it is also assumed that the mechanism for the equilibrium of the gases takes place through binary nucleon-nucleon collisions. Correspondingly a new set of master equation is obtained, the solution of which gives the proton and neutron occupation numbers.

2.5.3 The Exciton Model

The Exciton Model [1, 8] In the Exciton model, the compound nucleus states are characterized by the number of excited particles and holes (the excitons) at any stage of the nucleon-nucleon cascade. In this model the equilibration between target and projectile is achieved by the succession of nucleon nucleon interactions. An excited nucleus is considered as a gas of quasi-particles i.e., particle-hole degree of freedom is included.

The initial configuration is fixed by the nature of the projectile. For instance in case of a nucleon induced reaction, it is a two-particle-one hole configuration due to the interaction of the incident nucleon with a nucleon of the target which is excited from a state below to a state above the Fermi energy. Additional two-body interactions give rise to a sequence of states characterized by increasing exciton numbers, eventually leading to a fully equilibrated residual nucleus. Restriction to two-body interactions leads to the following selection rules concerning the possible variation of the number of particles, p , hole, h , and excitons, $n=p+h$,

In the course of the cascade of interactions: $\Delta p = 0, \pm 1$ $\Delta h = 0, \pm 1$ $\Delta n = 0, \pm 2$

The two possible sequences of events in the exciton model are:

i) The incident particle as well as the exited particle are all bound
 ii) The incident particle and one struck nucleon which attained a high energy are in the continuum. The exciton Model assumes that:

- 1) at each state of the cascade all the states with the same configurations and the same total energy are equiprobable.
- 2) At each state of the cascade all the processes which may occur are equiprobable.

2.5.4 The Hybrid Model

A decade ago predictions of pre-equilibrium decay in heavy ion reactions were made by using the hybrid model [8]. The H model for pre-equilibrium decay is formulated as:

$$\delta_{pec}(\epsilon) = \delta_{abs} \sum_{N=+2}^{n'} n = n_0 D_n p_v^n(\epsilon) \quad (2.14)$$

$p_v(\epsilon)$ is the emission probability of v with energy between ϵ and $\epsilon+d\epsilon$ from then exciton states. The pre-equilibrium decay probability is given by

$$p_v(\epsilon)d\epsilon = \sum_{N=+2}^{n'} n = n_0 \left[\frac{nx_n N_n(\epsilon, u)}{N_n(\epsilon)} \right] g d\epsilon \times \left[\frac{\lambda_c^n(\epsilon)}{\lambda_c(\epsilon) + \lambda_+(\epsilon)} \right] D_n \quad (2.15)$$

Where $p_v(\epsilon)d\epsilon$ is the number of particles of the type v emitted into the unbounded continuum with channel energy between ϵ and $\epsilon+d\epsilon$. The quantity in the first bracket of eq(2.15) represents the number of particles to be found (per Mev) at a given energy ϵ (with respect to continuum) for all scattering processes leading to an “n” exciton configuration. The nucleon-nucleon scattering energy partition function $N_n(\epsilon)$ is identical to the exciton state density $\rho_n(Eex)$ and $N_n(\epsilon)$ represent number of combinations with which n exciton may share Eex . The second set of bracket of eq(2.15) represents the fraction of the v type particles at energy ϵ which should undergo emission into the continuum, rather than making an inter-nucleon transition. The D_n represents the average fraction of the initial population surviving to the exciton number being treated.

In the hybrid model the probability of energy partitioning in the exciton state, n is borrowed from the HMB model. The HMB model determine the nucleon-nucleon interaction rate $\lambda+(\epsilon)$ from the free nucleon-nucleon scattering cross-sections to avoid the uncertainties associated with the values of $[M]^2$. The H model also calculates $\lambda+(\epsilon)$ from the nucleon-nucleon scattering cross-sections. But instead of experimental cross-sections it uses either Kikuchi-Kawai calculations or the empirical expression for the two-body interaction rate given by Blann by simplifying the detailed Kikuchi-Kawai calculations. The empirical expression is as follows:

$$\lambda_{\pm}^n = [1.4 \cdot 10^{21} (\epsilon + B_{sp}) - 6 \cdot 10^{18} (\epsilon + d_e + B_{sp})^2] k^{-1} \quad (2.16)$$

Where ϵ is the particle energy outside the nucleus i.e., ejectile energy and B_{sp} its separation energy k is an adjustable constant.

2.5.5 Geometry Dependent Hybrid Model

Geometry dependent hybrid (GDH) model [8] has been reasonably successful in reproducing a broad range of data. This was accomplished with several choices of parameter options. The geometry dependent hybrid model is a variant of the HM in which the nuclear geometry effects are considered. GDH model takes into account the reduced matter density and hence also the shallow potential. In this way the diffused surface properties sampled by higher impact parameter were incorporated into the pre-compound decay formalism in the geometry dependent hybrid model.

3. THE COMPUTER CODES AND FORMULATION

3.1 Analysis with computer codes

There are different computer codes to calculate the theoretical excitation functions. These are PACE4, CASCADE, ALIC-91 AND COMPLET codes. But as PACE4 code is appropriate for heavy ion induced reactions (from experience of different papers done) the excitation functions in this work are calculated by this code. For the sake of information the codes are described as follows:

Code CASCADE: This code is based on Houser-Feshbach theory. It does not consider the possibility of incomplete fusion(ICF) and PE emission. The decay probabilities are determined by the level densities of the daughter nuclei and the barrier penetrabilities for the various channels. The optical model potentials of Bechetti and Greenlees are used for calculated the transmission coefficients for protons and neutrons, and optical model potential of satcher is used for α -particles.

Code ALICE-91

The code ALIC-91 [16] developed by Blann, used to calculate the equilibrium (CN) as well as PE emission cross sections in light and heavy ion induced reactions. The CN calculations in this code are performed using Weisskopf-Ewing model. In this code the possibility of incomplete fusion is not taken in to account. The particles which could be emitted are neutrons, protons, deuterons or α -particles. The code may calculate the reaction cross sections for the residual nuclei up to 11 mass and 9 atomic number units away from the compound nucleus. Myers-Swiatecki/Lysekil mass formula is used for calculating Q-values and binding energies of all the nuclei in the evaporation chain. The inverse reaction cross sections used in the code are calculated using the optical model subroutines, although there is also an option of classical sharp cut of model. The transmission coefficients are calculated using the parabolic model of Thomas for heavy ions. Calculations for PF-emission in the code are done as summing equipartition of energy among the initial excited particles and holes. The mean free path(MFP) for intra nuclear transmission rates may be calculated either from the optical potential parameters of Bechetti and Greenlees or from pauli corrected nucleon-nucleon cross section. In the present calculations the optical potentials of Bechetti and Greenlees have been used. Level densities of the residue in

code ALICE-91 may be calculated either from the Fermi gas model or from the constant temperature form.

Couplet Code: The COMPLET code is a nuclear reactions code which was designed for versatility and ease of use in the bombarding energy range of a few Mev to Several hundred Mev. The code COMPLET is based same philosophy as the former code INDEX. It applies it applies the statistical model of compound nucleus decay developed by Weisskopf-Ewing and the hybrid and geometric dependent hybrid model of Blann and the further simplification and improvement by J.Ernst. It predicts the yield of residual nuclei in nuclear reaction with excitation energy up to 225Mev taking in to account two mechanisms. Pre-equilibrium emission is accompanied in the frames of the model of independently interacting exciton. Using this code it is possible to differentiate wheather the reaction if PE or CN using by changing exciton number. But the code if more effective in α -induced reaction than Heavy ion induced reactions.

3.1.1 Analysis with computer code PACE4

The Code PACE4 [12] is based on statistical approach. It is used for the compound Nucleus(CN) Formation. in this program the de-excitation of the Compound nucleus is followed by a Monte-Carlo procedure The decay sequence of an excited composite nucleus using the Houser-Feshbach formalism[12]. The angular momentum projections are calculated at each stage of de-excitation, which enables the de-excitation of the angular distribution of the emitted particles. The level density parameter is an important parameter which may be varied to match the experimental data. In this code the level density parameter a is given by:

$$a = \frac{A}{K}$$

Where A is the mass number of the compound nucleus and K is a free parameter. The value of k may be varied to match the experimental data. The effect of variation of the level density parameter K of this code on theoretical calculation of excitation functions for some isotopes of $^{165}_{67}\text{Ho}$, like $^{165}\text{Ho}(^6\text{O},3n)^{178}\text{Re}$, $^{165}\text{Ho}(^6\text{O},4n)^{177}\text{Re}$, $^{165}\text{Ho}(^6\text{O},5n)^{176}\text{Re}$ and

Ta family: $^{165}\text{Ho}(^6\text{O},\alpha n)^{176}\text{Ta}$, $^{165}\text{Ho}(^6\text{O},\alpha 2n)^{175}\text{Ta}$, $^{165}\text{Ho}(^6\text{O},\alpha 3n)^{174}\text{Ta}$, $^{165}\text{Ho}(^6\text{O},\alpha 4n)^{173}\text{Ta}$ and $^{165}\text{Ho}(^6\text{O},3\alpha 3n)^{166}\text{Tm}$. the experimental data were compared with PACE4 result for different values of k from 8-10 and 12, 14, and 15 with energy range of 72MeV to 105MeV. Default value of $k = 14$ gives satisfactory curve for the reactions, $^{165}\text{Ho}(^6\text{O},4n)^{177}\text{Re}$, $^{165}\text{Ho}(^6\text{O},5n)^{176}\text{Re}$, but for $^{165}\text{Ho}(^6\text{O},3n)^{178}\text{Re}$ it is not matching with the experimental value.

In the case of $^{165}\text{Ho}(^6\text{O},\alpha n)^{176}\text{Ta}$, $^{165}\text{Ho}(^6\text{O},\alpha 2n)^{175}\text{Ta}$, $^{165}\text{Ho}(^6\text{O},\alpha 3n)^{174}\text{Ta}$ and $^{165}\text{Ho}(^6\text{O},\alpha 4n)^{173}\text{Ta}$, the experimental value is above the theoretical curves. This may be b/c of ICF reaction. In the case of $^{165}\text{Ho}(^6\text{O},3\alpha 3n)^{166}\text{Tm}$, the theoretical curve is not seen in the graph as well as no tabular data. This is because of the residue is not produced in the considered energy range

4. Result and discussion

Table4.1: List of reactions identified along with the residues

Reaction	Residue
$^{165}\text{Ho}(^{16}\text{O},3n)$	$^{178}_{75}\text{Re}$
$^{165}\text{Ho}(^{16}\text{O},4n)$	$^{177}_{75}\text{Re}$
$^{165}\text{Ho}(^{16}\text{O},5n)$	$^{176}_{75}\text{Re}$
$^{165}\text{Ho}(^{16}\text{O},\alpha n)$	$^{176}_{73}\text{Ta}$
$^{165}\text{Ho}(^{16}\text{O},\alpha 2n)$	$^{175}_{73}\text{Ta}$
$^{165}\text{Ho}(^{16}\text{O},\alpha 3n)$	$^{174}_{73}\text{Ta}$
$^{165}\text{Ho}(^{16}\text{O},\alpha 4n)$	$^{173}_{73}\text{Ta}$
$^{165}\text{Ho}(^{16}\text{O},3\alpha 3n)$	$^{166}_{69}\text{Tm}$

In this work the excitation functions of eight residues of Ho were studied. The residues are:

$^{165}\text{Ho}(^{16}\text{O},3n)^{178}\text{Re}$, $^{165}\text{Ho}(^{16}\text{O},4n)^{177}\text{Re}$, $^{165}\text{Ho}(^{16}\text{O},5n)^{176}\text{Re}$, $^{165}\text{Ho}(^{16}\text{O},\alpha n)^{176}\text{Ta}$,
 $^{165}\text{Ho}(^{16}\text{O},\alpha 2n)^{175}\text{Ta}$, $^{165}\text{Ho}(^{16}\text{O},\alpha 3n)^{174}\text{Ta}$, $^{165}\text{Ho}(^{16}\text{O},\alpha 4n)^{173}\text{Ta}$ and $^{165}\text{Ho}(^{16}\text{O},3\alpha 3n)^{166}\text{Tm}$. It is
carried out using ^{16}O as projectile and ^{165}Ho as a target, at energy range of 72Mev to 105Mev.

The experimental excitation functions were compared with the theoretical predictions from PACE4 calculations. The experimental cross-section and energy are obtained from IAEA data source , EXFOR library[12, 3]

The projectile energy is measured in Mega electron volt(Mev) and the cross-sections are in mill barn(mb). Further explanation tables are given below.

Table 4.2. Theoretical and measured cross-sections for the reaction $^{165}\text{Ho}(^{16}\text{O},3n)^{178}\text{Re}$

E-lab (Mev)	δ_{expr} (mb)	δ_T (mb)				
		K=8	K=9	K=10	K=12	K=14
72.9 ± 1.86	50.33 ± 7.1	--	--	--	--	--
75	--	27	28.6	34.1	49.4	62.2
80	--	13.3	14.6	16.9	29.6	44.4
83.8 ± 1.72	36.97 ± 5.20	--	--	--	--	--
85	--	4.43	5.7	6.26	14.4	23.5
90	--	0.89	1.27	1.32	3.72	8.18
92.9 ± 1.60	6.67 ± 0.60	--	--	--	--	--
95	--	0.114	0.255	0.342	0.974	2.5
96.4 ± 0.80	0.84 ± 0.006	--	--	--	--	--
100	--	0.02	0.0502	0.0601	0.241	0.531
105 ± 0.78	--	--	0.0222	--	0.0111	0.133

In this reaction ^{178}Re is produced as residue from the reaction $^{165}\text{Ho}(^{16}\text{O},3n)^{178}\text{Re}$. In this case the reaction occurs via emission of (3n). Since there is no emission of α -particle is observed, we can say that this is the case of CF. here also experimental values are compared with theoretical PACE4 calculation results. PLD is also varied from 8-10, 12 and 14. For k =14, as can be seen in the graph, the curve is more approaching the experimental curve. Moreover, the experimental curve is associated with some energy errors.

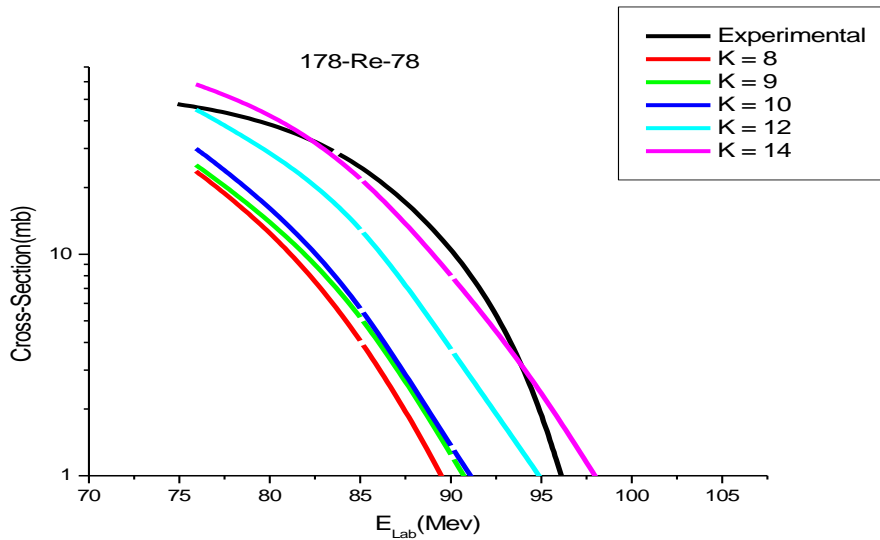


Fig.4.1 Excitation function for the $^{165}\text{Ho}(^{16}\text{O},3n)^{178}\text{Re}$ reaction

Table 4.3. Theoretical and measured cross-sections for the reaction $^{165}\text{Ho}(^{16}\text{O},4n)^{177}\text{Re}$

E-lab (Mev)	δ_{expr} (mb)	δ_T (mb)					
		K=8	K=9	K=10	K=12	K=14	K=15
72.9 ± 1.86	1.5 ± 6.0	--	--	--	--	--	
75	--	126	123	116	97.2	80.8	71.4
80	--	325	324	326	306	282	266
83.8 ± 1.72	393.6 ± 61.60	--	--	--	--	--	--
85	--	318	311	349	367	371	373
90	--	173	173	201	244	283	310
92.9 ± 1.60	373.2 ± 53.20	--	--	--	--	--	--
95	--	67.3	73.4	92.8	128	172	200
96.4 ± 0.80	247 ± 33.93	--	--	--	--	--	--
100	--	16.3	19.2	27.4	44.2	72.3	89.5
105 ± 0.78	103.9 ± 11.67	3.64	4.54	6.9	12.8	--	34.4

In the reaction $^{16}\text{O} + ^{165}\text{Ho}$, $^{177}\text{Re-75}$ is produced by emitting (4n) in the process. It is populated via emission of 4n from the excited composite nucleus $^{181}\text{Re}^*$ in the reaction. As shown in the table, The experimental values and theoretically calculated values of cross-section for the residue are listed. Since no α -particle emission is observed in this reaction, it is expected to be populated by CF only. The Experimental values are compared with theoretical PACE4 calculations with different PLD values from 8-10, 12,14, and 15. As it is seen in the graph below, The PACE4 calculation for $K = 15$ is relatively closer to the experimentally measured cross-section. Furthermore at energy from $\approx 75\text{Mev}$ to 85Mev , all the curves are closer enough to each other and also for $k = 15$, the curve is more coinciding with the experimental value in this range. At higher energy there is slight variation or gap. This may be because of direct reaction since this reaction is non- α emitting channel.

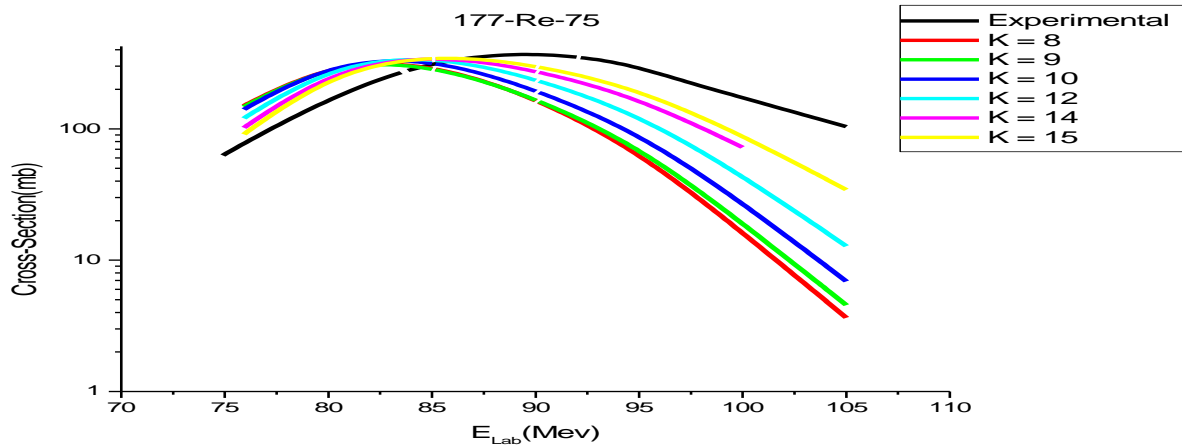


Fig.4.2 Excitation function for the $^{165}\text{Ho}(^{16}\text{O},4n)^{177}\text{Re}$ reaction

Table 4.4Theoretical and measured cross-sections for the reaction $^{165}\text{Ho}(^{16}\text{O},5n)^{176}\text{Re}$

E-lab (Mev)	δ_{expr} (mb)	δ_T (mb)			
		K=8	K=9	K=10	K=12
72.9 ± 1.86					
75					
80		19.8	14.3	4.99	2.82
83.8 ± 1.72	119.36 ± 18.0	--	--	--	--
85	--	200	197	149	106
90	--	478	467	427	357
92.9 ± 1.60	428.2 ± 61.20	--	--	--	--
95	--	597	590	580	533
96.4 ± 0.80	588.5 ± 90.30	--	--	--	--
100	--	470	477	491	540
105 ± 0.78	462.4 ± 73.20	254	276	287	387

Similarly in this case, in the reaction $^{165}\text{Ho}(^{16}\text{O},5n)^{176}\text{Re}$, the production of $^{176}_{75}\text{Re}$ is accompanied by the emission of (5n). Again as it can be seen from the graph below, for a free parameter K = 12, the PACE4 calculation is coinciding with the experimentally measured value. From ≈ 85 Mev to ≈ 100 Mev, the theoretical predictions are matching the experimental values. In general, The experimentally measured EFs for $^{178-176}\text{Re}$ evaporation residues expected to be populated via emission of xn (x = 3-5) from the excited composite nucleus $^{181}\text{Re}^*$. So in these channels, since there is no α -particle emission, and hence no possibility of ICF. Therefore these channels are expected to be populated by CF only. This is shown in Tables 5.1 to 5.3 and graphs 1 to 3.

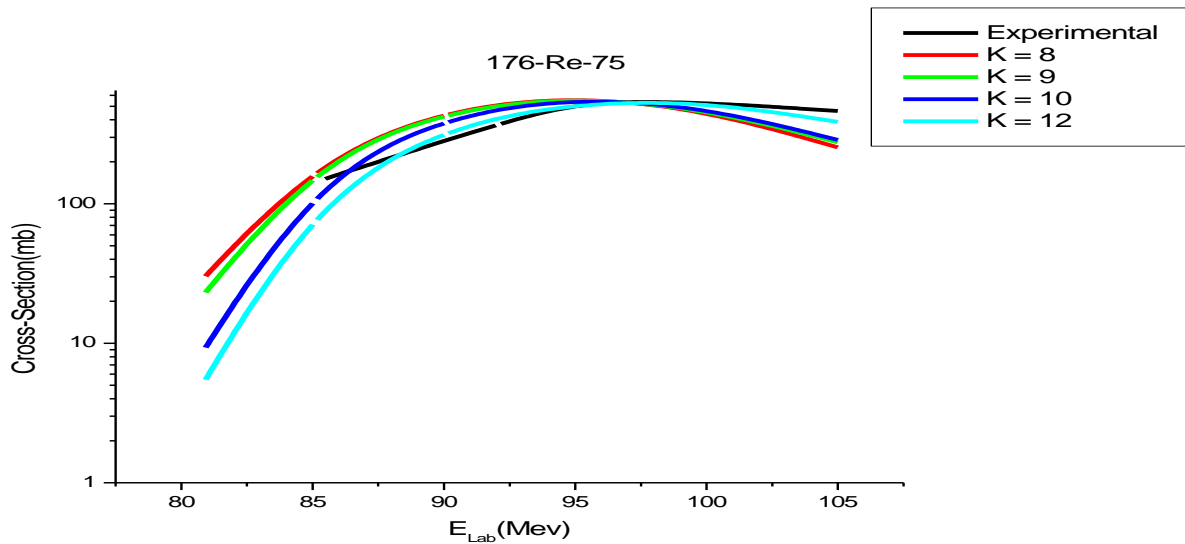


Fig.4.3 Excitation function for the $^{165}\text{Ho}(^{16}\text{O},5n)^{176}\text{Re}$ reaction

Table 4.5. Theoretical and measured cross-sections for the reaction $^{165}\text{Ho}(^{16}\text{O}, \alpha n)^{176}\text{Ta}$

E-lab (Mev)	δ_{expr} (mb)	δ_T (mb)			
		K=8	K=9	K=10	K=12
72.9 ± 1.86	--				
75	--	0.00162	0.00487	0.0227	0.0373
80	--	0.00382	0.0115	0.00382	0.0306
83.8 ± 1.72	22 ± 3.0	--	--	--	--
85	--	0.00572	--	0.0114	0.0114
90	--	0.0809	0.147	0.154	0.125
92.9 ± 1.60	34.7 ± 5.4	--	--	--	--
95	--	0.351	0.509	0.544	0.764
96.4 ± 0.80	42.07 ± 6.5	--	--	--	--
100	--	0.692	0.812	1.06	1.64
105 ± 0.78	76.4 ± 11.4	0.789	1.28	1.82	2.7

Reaction In the production of ^{176}Ta again α -particle emission is observed in the reaction $^{165}\text{Ho}(^{16}\text{O}, \alpha n)^{176}\text{Ta}$. It is populated by αn . Here again as the case of the other reactions, PACE4 calculation is compared with experimentally measured values for parameter of level density, K= 8-10, and 12. As it is seen in the other case still the experimental curve is above the theoretical PACE4 curve or they are far apart so we expect this also to be the case of ICF reaction. This can also be explained in two possible cases. Again this also may be because of ICF. i) CF of ^{16}O followed by the formation of an excited compound nucleus (CN) $^{181}\text{Re}^*$, from which evaporation of neutrons and the α -particles may take place. Or (ii) first ^{16}O breaks into α clusters in the nuclear force field of the ^{165}Ho another target such as ($\alpha + ^{12}\text{C}$) or ($^8\text{Be} + ^8\text{Be}$), and then one of fragments fuses with the target and the other fragment goes in to the forward cone elastically. In this case the excited composite system is less in mass and as that in the case of CF, hence referred to as ICF.

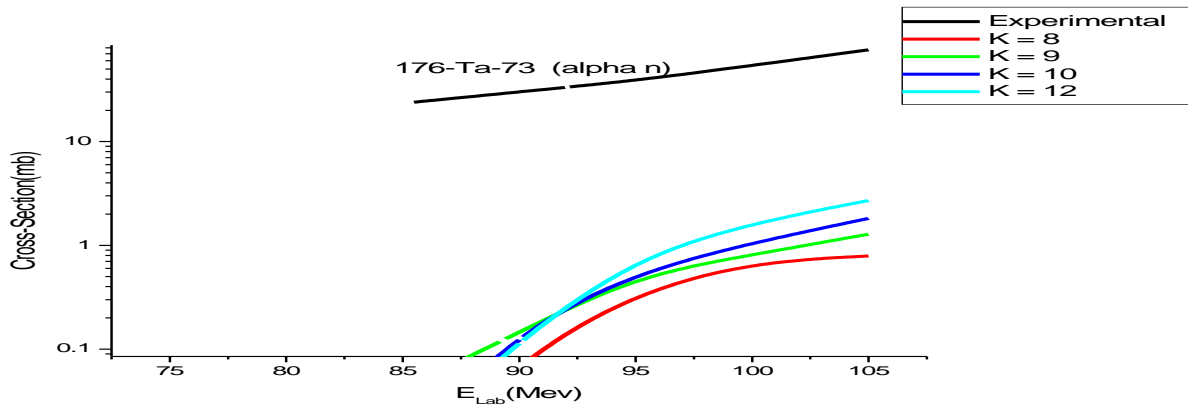


Fig.4.4 Excitation function for the $^{165}\text{Ho}(^{16}\text{O}, \alpha n)^{176}\text{Ta}$ reaction.

Table 4.6 Theoretical and measured cross-sections for the reaction $^{165}\text{Ho}(^{16}\text{O}, \alpha 2n)^{175}\text{Ta}$

E-lab (Mev)	δ_{expt} (mb)	δ_T (mb)			
		K=8	K=9	K=10	K=12
72.9 ± 1.86					
75		1.32	2.04	2.82	4.73
80		1.13	1.81	2.79	6.27
83.8 ± 1.72	2.09 ± 0.3	--	--	--	--
85	--	0.6	0.892	1.61	4.92
90	--	0.14	0.287	0.405	1.93
92.9 ± 1.60	15.16 ± 2.5	--	--	--	--
95	--	0.0615	0.0966	0.0966	0.579
96.4 ± 0.80	40.7 ± 6.0	--	--	--	--
100	--	0.15	0.14	0.1	0.2
105 ± 0.78	106.62 ± 15	0.722	0.8	0.766	0.789

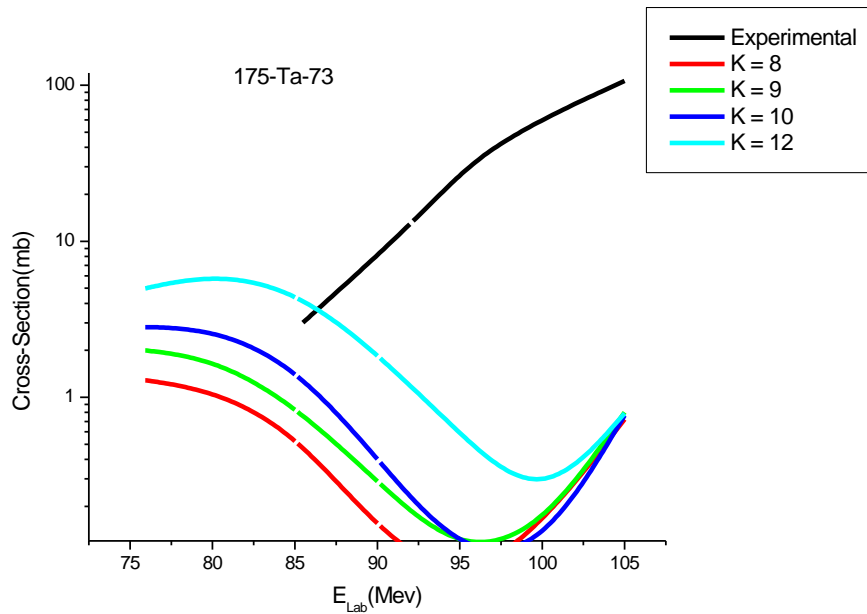


Fig.4.5 Excitation function for the $^{165}\text{Ho}(^{16}\text{O}, \alpha 2n)^{175}\text{Ta}$ reaction

For the production of ^{175}Ta , The reaction $^{165}\text{Ho}(^{16}\text{O}, \alpha 2n)^{175}\text{Ta}$ is populated by $(\alpha 2n)$. in this case theoretically calculated result(for LD = 8-10 and 12) and experimentally measured values are not matching. That is experimentally measured curve is above the theoretical one and they are far apart specially starting from projectile energy of $\approx 87.5\text{Mev}$. with this range the theoretical value is almost approaching zero. Here as it can be seen from the reaction that it is populated by $(\alpha 2n)$ and this may be because of incomplete fusion reaction of the projectile. i.e the projectile may break up in to $\alpha + ^{12}\text{C}$ before entering through the target.

Table 4.7. Theoretical and measured cross-sections for the reaction $^{165}\text{Ho}(^{16}\text{O}, \alpha 3n)^{174}\text{Ta}$

E-lab (Mev)	δ_{expr} (mb)	δ_T (mb)		
		K=8	K=9	K=10
72.9 ± 1.86				
75		1.38	1.28	1.35
80		6.97	9.01	9.83
83.8 ± 1.72	18.91 ± 2.27	--	--	--
85	--	13.8	18.3	22.7
90	--	12.3	17.7	24.4
92.9 ± 1.60	28.99 ± 4.05	--	--	--
95	--	7.97	11.2	16.2
96.4 ± 0.80	37.3 ± 4.10	--	--	--
100	--	3.08	4.49	6.59
105 ± 0.78	32.44 ± 4.80	0.711	1.48	2.14

Again in this reaction also ^{174}Ta is produced via emission of $\alpha 3n$. Tabular analysis is listed as shown. From the graph we see that experimentally measured values are above (far from) the theoretically measured excitation functions. Again in this case also PACE4 calculations are done for free parameter constant or parameter of level density (PLD) of 8-10, as the reaction is populated via α -particle emission, we expect that in this case ICF is responsible for the reaction.

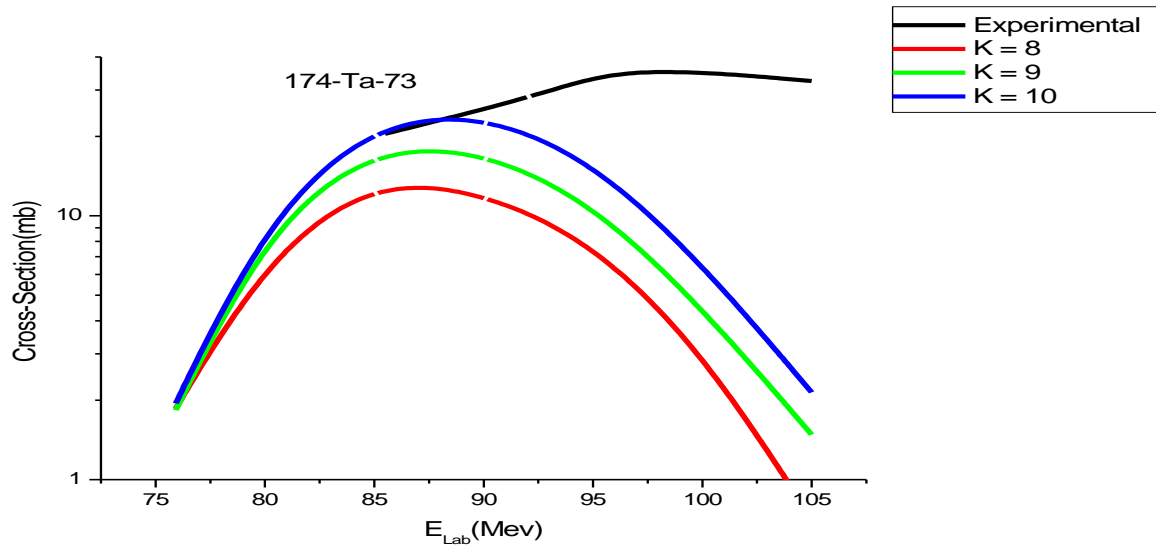


Fig.4.6 Excitation function for the $^{165}\text{Ho}(^{16}\text{O}, \alpha 3n)^{174}\text{Ta}$ reaction

Table 4.8. Theoretical and measured cross-sections for the reaction $^{165}\text{Ho}(^{16}\text{O}, \alpha 4n)^{173}\text{Ta}$

E-lab (Mev)	δ_{expr} (mb)	δ_T (mb)		
		K=8	K=9	K=10
72.9 ± 1.86	--			
75	--			
80	--	0.0879	0.0765	0.0191
83.8 ± 1.72	3.41 ± 05	--	--	--
85	--	2.91	2.68	2.09
90	--	15.4	16.4	16.7
92.9 ± 1.60	40.92 ± 4.5	--	--	--
95	--	32.6	39.8	44.1
96.4 ± 0.80	61.3 ± 8.00	--	--	--
100	--	41.4	52.6	64.7
105 ± 0.78	92 ± 12.30	37.3	49.1	63.9

Reaction that occurs via emission of α -particle emission is $^{165}\text{Ho}(^{16}\text{O}, \alpha 4n)^{173}\text{Ta}$. It is populated by $\alpha 4n$. Here again as the case of the other reactions, PACE4 calculation is compared with experimentally measured values for parameter of level density, K= 8-10. As it is seen in the other case still the experimental curve is above the theoretical PACE4 curve. Again this also may be because of ICF. That is, in such a case there may be two possible cases. i) CF of 16O followed by the formation of an excited compound nucleus(CN) $^{181}\text{Re}^*$, from which evaporation of neutrons and the α -particles may take place. Or (ii) first ^{16}O breaks into α clusters in the nuclear force field of the ^{165}Ho another target such as ($\alpha + ^{12}\text{C}$) or ($^8\text{Be} + ^8\text{Be}$), and then one of fragments fuses with the target and the other fragment goes in to the forward cone elastically. ICF is explained in the same sense as this work in [12,13] In this case the excited composite system is less in mass and as that in the case of CF, hence referred to as ICF.

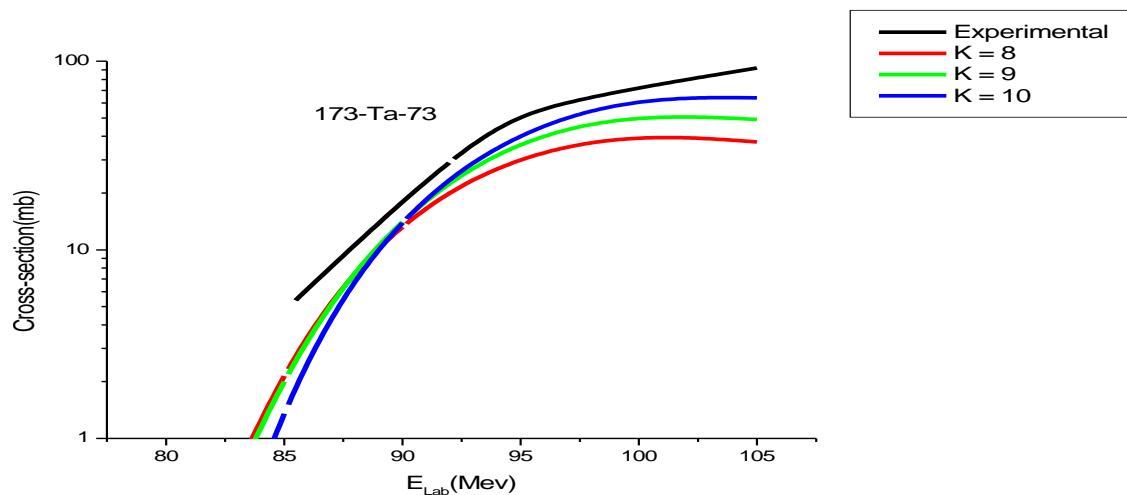


Fig.4.7 Excitation function for the $^{165}\text{Ho}(^{16}\text{O}, \alpha 4n)^{173}\text{Ta}$ reaction

Table 4.9. Theoretical and measured cross-sections for the reaction $^{165}\text{Ho}(^{16}\text{O}, 3\alpha 3n)^{166}\text{Tm}$

$E_{\text{Lab}}(\text{Mev})$	$\delta_{\text{Expt}}(\text{mb})$	$\delta_T(\text{mb})$			
		K=8	K=9	K=10	K=12
72.9 ± 1.86					
75		-	-	-	-
80		-	-	-	-
83.8 ± 1.72	7.62 ± 1.14				
85	--	-	-	-	-
90	--	-	-	-	-
92.9 ± 1.60	12.5 ± 1.88				
95	--	-	-	-	-
96.4 ± 0.80	24.59 ± 3.7				
100	--	-	-	-	-
105 ± 0.78	36.67 ± 5.55	-	-	0.0111	-

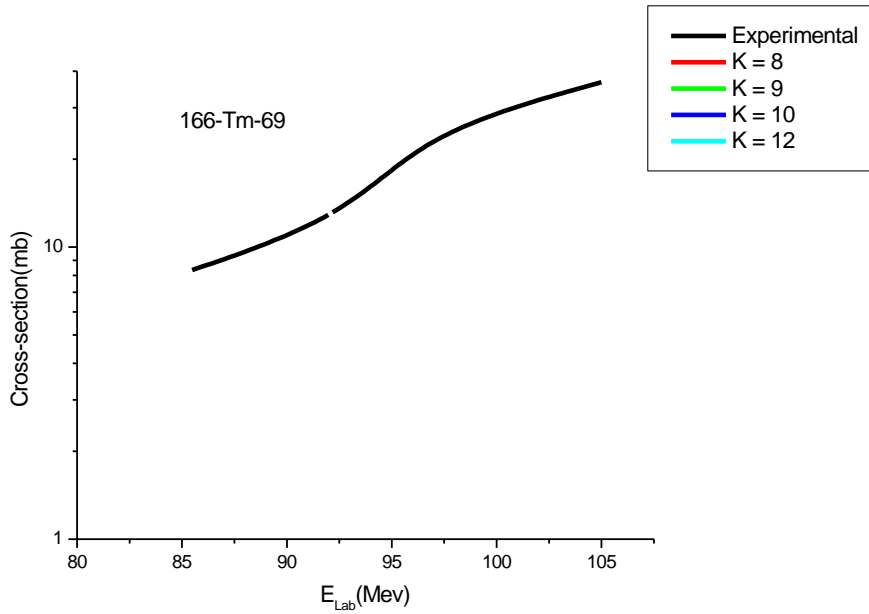


Fig.4.8 Excitation function for the $^{165}\text{Ho}(^{16}\text{O}, 3\alpha 3n)^{166}\text{Tm}$ reaction

Experimentally measured EFs of $^{166}\text{Tm}(3\alpha 3n)$ are shown, while PACE4 predictions are not there (even the residue is not produced in the considered energy range) and hence are not shown in the graph. This result is similarly explained in the paper [12]. In this work, Only one result is displayed and indicated on the table, but the others couldn't be seen on the graph.

Generally for α -particle emitting reactions, The experimentally measured and theoretically calculated EFs for the α xn channels such as $^{177-x}\text{Ta}$ (where $x = 1-4$) and EFs for ^{166}Tm are shown in graphs 4 to 8. To identify Suitable LDP for the analysis of α -emitting channels, different values of the free parameter (That is $K = 8-10$ and 12) have been tested. As can be seen from the graphs, the theoretical predictions with input parameters are very similar and show very small change at relatively higher projectile energies. It may however, be pointed out that a value of $K \geq 10$ may give rise to anomalous effect in particle multiplicity and compound nucleus temperature so more suitably the free parameter value of $k = 8$ is has been adopted in this work.[12]. and then the same is done in this work as well.

5. Conclusion

As it is discussed in this work, the excitation functions for (O,3n), (O,4n), (O,5n), (O, α n), (O, α 2n), (O, α 3n), (O, α 4n), and (O, 3α 3n), reactions for $^{16}\text{O} + ^{165}\text{Ho}$ have been studied in the energy range between 72MeV to 105MeV. The comparative study of the experimentally measured excitation functions with the theoretically calculated PACE4 predictions show that, for non α -particle emitting channels, the theoretically calculated values agree with the experimentally measured cross-sections for chosen level density parameter value (of course the parameter value is not the same for all the channels). Here, what has to be taken in to consideration is that, the experimental values associated with some errors because of different factors[12]. In such a case we expect that the projectile is completely fused in to the target(or no breaking before entering) and hence it is populated with complete fusion (CF) reaction [12]. This observed for Re family: ^{178}Re , ^{177}Re , and ^{176}Re . these are produced as it is discussed before, by evaporation or emission of 3, 4 and 5 neutrons from the compound nucleus(composite system) $^{181}\text{Re}^*$.

For the reactions that are populated α xn(x = 1-4) and 3α 3n the theoretical predictions are not matching with the experimental curves. Or the experimentally measured cross-section values are higher than the theoretical results. This can be expected for breaking reactions. That is the projectile may be broken in to α and ^{12}C or in to $^8\text{Be} + ^8\text{Be}$ before entering through the target by the coulomb interaction(at lower projectile energy). Or the projectile breaking may also be observed after entering in to the target(for high energy of projectile). This happens when the projectile is coming with higher energy. So In this case (in cases of α -particle emission)we can say that this may be because of incomplete fusion (ICF) reaction[12]. $^{177-x}\text{Ta}$ (where x = 1-4) and ^{166}Tm are populated with α -particle emission and are in such a category. So it may be possible to conclude that complete fusion, incomplete fusion and pre-equilibrium emission processes play important roles in the reactions induced by heavy ions.

References

1. P.E.Hodgson, E.Gadioli and E.GadioliErba, Introductory Nuclear Physics, Oxford University Press, 2003.
2. J.P. Lestone, phys.Rev.C 53, 2014(1996)
3. Exfor library: <http://www.mndc.bnl.gov/exfor>
4. N. Bohr, Nature, 137, 344, (1936)
5. S.N Ghoshal, phys. Rev. 80, 939 (1950)
6. Unnati, M.K.Sharma, B.P.Singh, S.Gupta, H.D.Bhardwaj, A.K.Sinha, International Journal of Modern Physics E,2005.
7. C.A. BERTULANI, Department of Physics, Texas A&M University, Commerce, TX 75429, USA
8. K.F.Amanuel, PHD thesis, Addis Ababa University, Addis Ababa, Ethiopia, 2011
9. M.K.Sharma, Unnati, B.K.Sharma, B.P.Singh, H.D.Bhardwaj, R.Kumar, K.S.Golda, And R.Prasad,Physical Review 70, 2004.
10. J.S.Lilley, Nuclear physics principles and Applications, John Wiley&Sons Ltd, 2001
11. B. Bindu Kumar nad S. Mukherjee, Physical review C57, 1998.
12. Kamal Kumar,TauseefAhamad ,Sabir Ali, I.A. Riziv, AvinashAgarwal, R. Kumar, K.S.Golda, and A.K. Chaubey. Physical Review C 87, 044608(2013)
13. AvinashAgarwal, Sunil Dutt, Anjali Sharma, I.A. Riziv, Kamal kumar, Sabir Ali, TauseefAhamad, Rakesh Kumar, and A.K. Chaubey.International J. of modern physics, E38, 17001(2012)
14. The Stopping and Range of Ions in Matter (SRIM) code:
[<http://www.srim.org/SRIM/SRIMLEGL.htm>].
15. Walter E.Meyerhof, Elements of Nuclear Physics, McGraw-Hill,Inc, 1967.
16. M.Blann,phys. Rev.Letts.28,757(1972)

Declaration

This thesis is my original work, has not been presented for a degree in any other University and that all the sources of material used for the thesis have been fully acknowledged.

Name: TesfahunMarkos

Signature: _____

Place and time of submission: Addis Ababa University, 2014

This thesis has been submitted for examination with my approval as University advisor.

Name: Prof.A.K. Chaubey

Signature: _____